Since January 2020 Elsevier has created a COVID-19 resource centre with free information in English and Mandarin on the novel coronavirus COVID-19. The COVID-19 resource centre is hosted on Elsevier Connect, the company's public news and information website.

Elsevier hereby grants permission to make all its COVID-19-related research that is available on the COVID-19 resource centre - including this research content - immediately available in PubMed Central and other publicly funded repositories, such as the WHO COVID database with rights for unrestricted research re-use and analyses in any form or by any means with acknowledgement of the original source. These permissions are granted for free by Elsevier for as long as the COVID-19 resource centre remains active.

Antiviral Research 106 (2014) 33–41

Contents lists available at ScienceDirect

Antiviral Research

journal homepage: www.elsevier.com/locate/antiviral

Triggering unfolded protein response by 2-Deoxy-D-glucose inhibits porcine epidemic diarrhea virus propagation

Yue Wang [a], Jia-rong Li [a], Ming-xia Sun [a], Bo Ni [a], Changchao Huan [a], Li Huang [a], Chen Li [a], Hong-jie Fan [a,c], Xiao-feng Ren [b,*], Xiang Mao [a,*]

[a] College of Veterinary Medicine, Nanjing Agricultural University, 1 Weigang, Nanjing, Jiangsu Province, 210095, China
[b] College of Veterinary Medicine, Northeast Agricultural University, 59 Mucai Street, Harbin, Xiangfang District, 150030, China
[c] Jiangsu Co-innovation Center for Prevention and Control of Important Animal Infectious Diseases and Zoonoses, Yangzhou, 225009, China

ARTICLE INFO

Article history:
Received 12 November 2013
Revised 5 March 2014
Accepted 16 March 2014
Available online 25 March 2014

Keywords:
Porcine epidemic diarrhea virus
Endoplasmic reticulum stress
Unfolded protein response
2-Deoxy-D-glucose
Antiviral

ABSTRACT

The unfolded protein response (UPR) is cyto-protective machinery elicited towards an influx of large amount of protein synthesis in the endoplasmic reticulum (ER). Extensive studies suggest that the UPR can also be activated during virus infection. In the present studies, we first evaluated if porcine epidemic diarrhea virus (PEDV) infection activated the UPR pathways. Electron microscopy analysis demonstrated the morphology changes of ER post-PEDV infection. Western blot and real-time PCR identified the differences of UPR genes in response to PEDV infection. The results suggested that PEDV infection induced UPR in Vero cells. Meanwhile, we silenced the expression of PKR-like ER kinase (PERK) by shRNA, we found that the knockdown of PERK increased virus loads in the cells, which was consistent with the result on 4-phenylbutyrate (4-PBA) treatment. We next determined whether 2-Deoxy-D-glucose (2-DG), an ER stress inducer, possessed antiviral activity against PEDV infection. Plaque formation assay, RT-PCR and Western blot analysis suggested that 2-DG might inhibit virus infection by affecting viral protein translation during the early stage of virus infection. Interestingly, we also found that 2-DG treatment could affect virus assembly, which is similar to previous studies on influenza virus. All these results support the therapeutic potential of using 2-DG or glucose/mannose analogs to induce the UPR to block virus replication.

© 2014 Elsevier B.V. All rights reserved.

1. Introduction

Porcine epidemic diarrhea (PED) is first found among English feeder and fattening pigs in 1971 (Wood, 1977). It is a devastating enteric disease that manifests as sporadic outbreaks during winter. PEDV is the causative agent of PED and causes severe enteritis, vomiting and watery diarrhea, resulting in a high mortality in piglets. Since 2013, PEDV spreads rapidly in swine farms in the United States, causing significant economic loss (Huang et al., 2013; Mole, 2013). PED is now becoming one of the most important swine diseases causing great economic loss and public health concerns.

PEDV was first reported in Belgium and the United Kingdom (Pensaert and De Bouck, 1978). PEDV belongs to the family of coronavirus and is classified into group I of the genus *Coronavirus*. Its size ranges in diameter from 95 nm to 190 nm, including its projection. The viral replicase is encoded by ORF1a and ORF1b (Kocherhans et al., 2001). The viral structural proteins include spike protein, envelope protein, membrane protein and nucleocapsid protein (Song and Park, 2012). The virus also encodes an accessory protein, ORF3a, which has been suggested as an important virulent determinant of this virus (Park et al., 2011).

The unfolded protein response (UPR) is a cellular stress response induced by the accumulation of misfolded or unfolded proteins within the endoplasmic reticulum (ER) in order to initiates a number of cellular responses to restore ER homeostasis. The primary function of UPR is for stress adaptation and cell survival. The UPR can also be induced through glycosylation inhibitors treatment (e.g., tunicamycin), calcium homeostasis changes, nutrient depletion, overexpression of abnormal proteins, or virus infection (Dorner et al., 1989). UPR is represented by a marked increase of ER-localized proteins such as glucose-regulated protein 78 (GRP78/BiP) or 94 (GRP94). UPR is controlled by three main signaling pathways, including inositol-requiring enzyme 1 (IRE1), activating transcription factor 6 (ATF6) and PKR-like ER kinase (PERK). In non-stressed cells, GRP78 binds to PERK, IRE1 and ATF6 to keep them in an inactive form (Bertolotti et al., 2000).

* Corresponding authors. Tel.: +86 451 55191974 (X.-f. Ren), +86 25 84399865 (X. Mao).
E-mail addresses: rxfemail@gmail.com (X.-f. Ren), xmao@njau.edu.cn (X. Mao).

http://dx.doi.org/10.1016/j.antiviral.2014.03.007
0166-3542/© 2014 Elsevier B.V. All rights reserved.

IRE1 is an ER transmembrane protein that contains endoribonuclease and cytoplasmic protein kinase domains. ER stress can induce the activation of IRE1. Activated IRE1 removes 26 nucleotides from the mRNA of X-box binding protein 1 (XBP-1) to generate a spliced mRNA encoding the functional XBP-1(s) protein (Yoshida et al., 2003). PERK, an ER resident serine/threonine protein kinase, can phosphorylate the -subunit of eukaryotic translation initiation factor 2 (eIF2α). During UPR, the release of GRP78 from PERK results in the homodimerization of PERK, causing phosphorylation of eIF2α to impair protein translation (Fernandez et al., 2002; Liu et al., 2009). ATF6 normally anchors in the ER membrane. GRP78 release exposes a Golgi localization signal on ATF6. After translocation to the Golgi, ATF6 precursor (p75ATF6) is further processed into its active form (p50ATF6), which enters the nucleus to activate the transcription of UPR target genes (Ye et al., 2000).

Many enveloped DNA and RNA viruses infection can induce the UPR in mammalian cells (Zhang and Wang, 2012). For example, studies on hepatitis C virus (HCV) show that HCV infection induces the UPR, which can activate the autophagic pathway to promote HCV RNA replication in human hepatoma cells (Ke and Chen, 2011). Some viruses regulate the UPR to initiate an environment more favorable for their replication (Buchkovich et al., 2009, 2008). African swine fever virus (ASFV) uses the endoplasmic reticulum (ER) as a site of replication. ASFV infection triggers ER stress and the unfolded protein response (UPR) in the host cells by inducing ATF6 signaling pathway of the UPR, but not PERK or IRE1 pathway. UPR regulation by ASFV might prevent early apoptosis to facilitate viral replication (Galindo et al., 2012). Tick-borne encephalitis virus infection activates the IRE1 and ATF6 signal pathways (Yu et al., 2013). A study on severe acute respiratory syndrome associated coronavirus (SARS-CoV) identified one of accessory proteins of SARS-CoV (8ab protein) binds directly to the luminal domain of ATF6, suggesting 8ab protein might facilitate protein folding and processing by modulating UPR (Sung et al., 2009). This finding suggests that some viruses might use their own protein(s) to regulate UPR response.

The glucose analog, 2-Deoxy-D-glucose (2-DG), can be used to block or probe sugar metabolism in cancer cells (Kurtoglu et al., 2007a). Because of its mannose-like structure, 2-DG can compete with mannose in the growing oligosaccharide chain during the initial steps of N-linked glycosylation occurring in the ER (Kurtoglu et al., 2007b). Oligosaccharide chains incorporated with 2-DG cannot form the functional $glucose_3$ $mannose_9$ moiety for proper protein glycosylation. Abnormal N-linked glycosylation interferes with protein folding and induces ER stress to activate UPR, which results in the inhibition of protein synthesis. It has been reported that 2-DG can inhibit the replication and gene expression of Kaposi's Sarcoma-Associated Herpesvirus (Leung et al., 2012). 2-DG also inhibits influenza virus infection (Nakamura and Compans, 1978). Thus, we proposed that UPR induced by 2-DG would counter the ability of PEDV to circumvent UPR-mediated blockage of protein synthesis, thereby impairing PEDV gene expression and resulting in inhibition of viral replication.

In these studies, we demonstrated that PEDV infection can induce UPR. We showed an interaction between UPR and the replication of PEDV. As expected, we revealed that 2-DG induced UPR leads to the inhibition of viral replication in Vero cells. Our results provide new antiviral insights that may be applicable to inhibit the replication of PEDV in clinic.

2. Materials and methods

2.1. Cell and virus

Porcine epidemic diarrhea virus (strain HLJBY) was propagated in Vero cells in the presence of 60 μg/ml trypsin cultured in DMEM supplemented with 10% fetal bovine serum (Invitrogen, China). To obtain replication-incompetent PEDV, 10 ml aliquots of virus were dispersed in culture medium (10 cm tissue culture dish) and exposed UV light (254 nm) for 2 h on ice. Following the exposure, the samples were harvested and stored at −80 °C. The absence of virus infectivity after UV irradiation was confirmed by plaque formation assay and Q-PCR as described below (Jheng et al., 2010).

2.2. Chemicals, antibodies and other reagents

2-Deoxy-D-glucose (2-DG), tunicamycin (Tu), 4-phenylbutyrate (4-PBA), anti-β-actin antibody were purchased from Sigma–Aldrich. The following rabbit primary antibodies were purchased from Cell Signaling: PERK, phospho-PERK, eIF2α, phospho-eIF2α, GRP78. Rabbit primary antibody ATF6 was purchased from Santa Cruz. The polyclonal antibody for PEDV N was generated previously in our lab. The PERK shRNA designed specifically to knockdown PERK expression was purchased from Genepharma (Shanghai, China) along with the control shRNA.

2.3. Cell culture, virus infection and plaque formation assay

According to the requirement of different experiments, Vero cells were either infected with PEDV (MOI of 0.01, 0.1 or 1) or mock-infected with phosphate-buffered saline (PBS). After 1 h incubation in 37 °C, unbounded viruses were removed by washing the cells thrice with PBS and the cells were cultured in DMEM supplemented with 2% FBS at 37 °C for different time. For 2-DG treatment experiments, Vero cells were pretreated with varying concentrations of 2-DG for 24 h before virus infection (MOI = 0.01). The cells were infected with PEDV at 37 °C for 2 h, the unbounded viruses were removed by washing thrice with PBS and cultured in DMEM supplemented with 2% FBS and varying concentrations of 2-DG at 37 °C for 24 h. For 4-PBA treatment experiments, Vero cells were first infected with PEDV (MOI = 0.01) for 2 h at 37 °C, unbounded viruses were removed by washing thrice with PBS. Then cells were cultured in DMEM supplemented with 2% FBS and varying concentrations of 4-PBA at 37 °C for 48 h.

For virus entry study, the cells were incubated with PEDV for 1 h (MOI = 1) at 4 °C. The cells were washed three times with PBS, then incubated with DMEM supplemented with 2% FBS at 37 °C. 30 min later, the cells were washed twice with a low pH buffer (40 mM citric acid, 10 mM KCl, 135 mM NaCl, pH 3.0) for 30 s to inactivate or remove the bound viruses that did not penetrated the cells. The cells were then washed twice with PBS for further experiments (Hancock et al., 2010).

For plaque formation assay, viral culture supernatants with 10-fold dilutions (from 10^2 to 10^5) were added into 6-well plate with confluent monolayer of Vero cells. The plate was then incubated at 37 °C for 2 h with gentle agitation at every 15-min interval. The excess virus inocula were removed by rinsing the wells with PBS for three times. Subsequently, overlay medium (2% low melting-point agarose with DMEM medium containing 2% FBS) was added to each well and the plates were further incubated at 37 °C with 5% CO_2 for 3 days. The cells were stained with 0.5% crystal violet.

2.4. Western blot analysis

The cells in 6-well plate were washed with PBS for three times, scraped from the culture plate, and lysed with the cell lysis buffer (50 mM Tris–HCl, pH 7.4, 150 mM NaCl, 1% Triton X-100, 2 mM EDTA, 0.1% SDS, 5 mM sodium orthovanadate) containing a protease inhibitor cocktail (Roche Molecular Biochemicals) and 0.1 mM PMSF for 2 h. The cell lysates were centrifuged at 14,000*g* for 20 min at 4 °C. Protein concentration was determined using the

Bradford assay. Equal amount of protein samples were loaded and separated on SDS–PAGE. The proteins in the gel were transferred to polyvinylidene fluoride (PVDF) membranes (Bio-Rad, USA) which were then blocked with 5% nonfat dry milk in PBST at 4 °C overnight and incubated for 2 h with different primary antibodies. Following this, the membrane was incubated for 1 h with the appropriate secondary antibodies. Immunoreactive bands were visualized by an enhanced chemiluminescence system (Amersham). The western bands were quantified by densitometric analysis using NIH ImageJ software. The results represent the mean data from three independent experiments. $^{*}p < 0.05$.

2.5. Transmission electron microscopy analysis

For conventional ultrastructural analysis, Vero cells were either mock-infected or infected with PEDV at MOI of 0.1 for 12, 24, 36 and 48 h, respectively. The cell samples were then processed as previously described (Rutkowski et al., 2006). Ultra-thin sections were viewed on a Hitachi H-7650 transmission electron microscope (Hitachi Ltd.).

2.6. Flow cytometry

Detached Vero cells were washed once with PBS, fixed with 4% paraformaldehyde for 15 min at room temperature, and stained with rabbit anti-human CD13 protein (Boster Bio-Tech Co. Ltd., Wuhan, China) for 1 h at 4 °C. The cells were washed with PBS and incubated with Fluorescein (FITC)-conjugated AffiniPure Goat Anti-Rabbit IgG (H + L) (Boster Bio-Tech Co. Ltd., Wuhan, China) for 30 min. Unbound secondary antibody was washed away with PBS. The cells were resuspended in 200 μl PBS, and analyzed on a FACSCalibur cytometer (Becton Dickinson Immunocytometry Systems). At least 10,000 cells were analyzed for each sample.

2.7. RNA interference

Vero cells were grown to 60–70% confluence in six-well cell culture plates and then transiently transfected with indicated interfering RNA (shRNA) plasmids using TransFast Transfection Reagent (Promega, Shanghai) according to the manufacturer's instructions. The silencing efficiency of the shRNA was detected by Western blot analysis. The scramble shRNA was used as negative controls.

2.8. RT-PCR

The total RNA was extracted from the Vero cells with TRIzol reagent (Invitrogen) and purified according to the manufacturers' recommendations. Intracellular PEDV and Vero cells genome levels were quantified with the SYBR Green Probe 3-step QRT-PCR kit (Takara, China) and fluorescent quantization meter (ABI PRISM 7300 sequence detection system, Applied Biosystems). For cDNA preparation, total RNA (1 μg) was reverse transcribed with first strand cDNA synthesis kit (Takara, China). Triplicate cDNA samples were amplified with the RT-PCR kit. The primer for UPR pathway genes are described in Table 1. RT-PCR analysis for XBP-1 were carried out using the SuperScript One Step RT-PCR kit (Invitrogen), following the manufacturers' instructions. The primers used were: forward primer: 5′-CCTTGTAGTTGAGAACCAGG-3′ and reverse primer 5′-GGGGCTTGGTATATATGTGG-3′. Amplification condition included an initial step of 45 °C for 30 s, followed by a denaturation step of 94 °C for 2 min, 30 cycles of 94 °C for 30 s, 55 °C for 30 s and 70 °C for 30 s (Galindo et al., 2012). PCR products were resolved by electrophoresis in a 2% agarose gel and stained with GoldenView.

Table 1
Primers used for real time PCR.

Target gene	Primer sequence
GRP94	Forward-TCCGCCTTCCTTGTAGCAGATA
	Reverse-TTGTCGTTCCCCGTCCTAGA
GRP78	Forward-ACCGCTGAGGCTTATTGGG
	Reverse-TGCCGTAGGCTCGTTGATG
CALN	Forward-TCCTTGAAGCAAATGTGTGG
	Reverse-ACTGTCAACGGAGGGTGAAG
PDI	Forward-CCGAAGATTTTTGGAGGTGA
	Reverse-TGCTCAGTTTGCCGTCATAG
CALR	Forward-CGAGGACTGGGATGAAGAGA
	Reverse-AATCTGGGTTGTCGATCTGC
ERP57	Forward-CCTAAAAGCAGCCAGCAACT
	Reverse-TGCCACAGTCTTGTCCTCAA
CHOP	Forward-GCCTTTCTCCTTTGGGACACTGTCCAGC
	Reverse-CTCGGCGAGTCGCCTCTACTTCCC
GADD34	Forward-GGAGGAAGAGAATCAAGCCA
	Reverse-TGGGGTCGGAGCCTGAAGAT
$p58^{IPK}$	Forward-CTCAGTTTCATGCTGCCGTA
	Reverse-TTGCTGCAGTGAAGTCCATC
ATF4	Forward-AAGCCTAGGTCTCTTAGATG
	Reverse-TTCCAGGTCATCTATACCCA
EDEM	Forward-TTGACTCTTGTTGATGCATTGGA
	Reverse-GCTTTCTGGAACTCGGATGAAT
GAPDH	Forward-AGGTCGGAGTCAACGGATTT
	Reverse-TAGTTGAGGTCAATGAAGGG
PEDV ORF3	Forward-TTTGCACTGTTTAAAGCGTCT
	Reverse-AGTAAAAGCAGACTAAACAAAGCCT
PEDV N	Forward-GCACTTATTGGCAGGCTTTGT
	Reverse-CCATTGAGAAAAGAAAGTGTCGTAG

2.9. Cytotoxicity assay

Approximately 1×10^5 Vero cells per well were seeded in a 96-well cell culture plate and cultured for 20 h at 37 °C in the presence of 5% CO_2. The medium was replaced with fresh DMEM supplemented with 2% FBS containing either Tu (2 μg/ml), 2-DG (10 mM) or 4PBA (5 mM), and the plates were incubated for up to 24 or 48 h. The cytotoxicity of PERK depletion was assayed by measuring lactate dehydrogenase (LDH) release from cells with Cytotox-One homogenous membrane integrity kit (Promega, USA) according to the manufacturers' instructions. Our result demonstrated that the viability of Vero cells was not significantly affected after Tu (2 μg/ml), 2-DG (10 mM) or 4-PBA (5 mM) treatment or shPERK transfection (data not shown).

2.10. Statistical analysis

All data were determined in triplicate and are representative of at least two separate experiments. The results represent the means ± standard deviations of triplicate determinations. The differences between means were considered significant at $^{*}p < 0.05$, very significant $^{**}p < 0.01$. All statistical analyses were performed by one-way ANOVA using a SPSS 16.0 software package (version 16.0, SPSS Inc., Chicago, IL, USA).

3. Results

3.1. PEDV infection can induce ER morphology changes

To investigate whether PEDV infection elicited an ER stress response, the transmission electron microscopy (TEM) analysis was performed to determine whether PEDV induced the endoplasmic reticulum hypertrophy. We observed the ER morphology was impressively deranged with hyper-swollen membranes throughout the majority of PEDV-infected cells. When viewed in sagittal section, multiple large vesicles appeared to be surrounded by the swollen ER (Fig. 1B and C), some of which were also full of virions

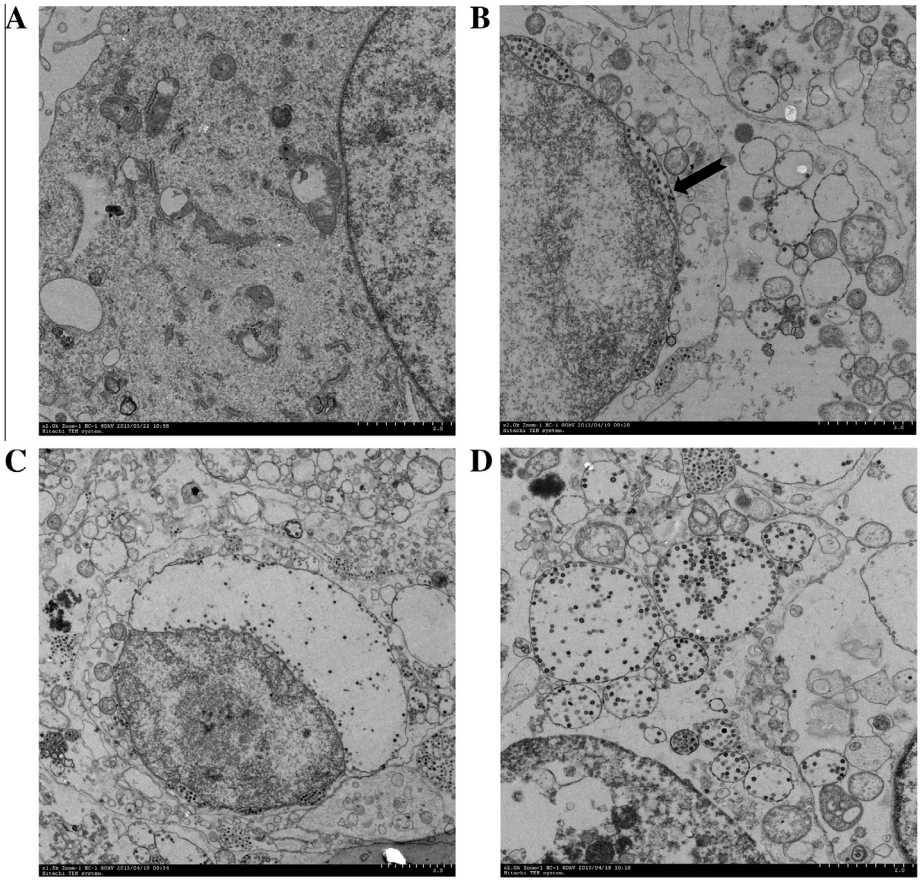

Fig. 1. The transmission electron microscopy analysis of PEDV-infected cells. Vero cells were mock infected or infected with PEDV at MOI of 0.1 for 24 h. The cells were fixed and processed for electron microscopy analysis. (A) Mock infected Vero cells. (B) PEDV-infected Vero cells. The arrow indicated the swollen endoplasmic reticulum. (C) The swollen endoplasmic reticulum closed to nuclei in infected cells. (D) The vesicles full of virions.

(Fig. 1D). PEDV particles are mostly spherical, and have an average diameter of ~120 nm. Similar phenomenon was rarely observed in the uninfected cells, whose cytoplasm were dense and contained morphologically normal organelles (Fig. 1A). We concluded that the PEDV infection in Vero cells could induced the ER membrane structure changes.

3.2. PEDV infection activates the host cellular UPR signaling pathways

To explore whether PEDV infection activated cellular UPR signaling pathways, we then examined the major components of UPR signaling pathways during the infection. Vero cells were mock-infected or infected with PEDV (Tu, an inhibitor of N-linked glycosylation which causes accumulation of underglycosylated unfolded proteins in the ER lumen, was used as the control) at MOI of 0.01. The cells were harvested at the indicated time post infection. Cell lysates were analyzed by Western blot using specific antibodies against UPR signal pathway marker proteins. As shown in Fig. 2A, the expression level of GRP78 increased significantly from 12 h to 48 h in virus infected cells compared with the mock infected control. Western blot showed that phosphorylated-PERK and phosphorylated-eIF2α expression levels were significantly higher than that in mock-infected cells at 12 h (Fig. 2B and C). Our data confirmed that PEDV infection results in endoplasmic reticulum stress in the cells (Xu et al., 2013a,b). To determine whether PEDV infection were sufficient to activate the ATF6 pathway, Western blot was performed to investigate the processing of ATF6 during PEDV infection. The result showed that the p75ATF6 decreased and p50ATF6 appeared at 24 h (Fig. 2D), suggesting that PEDV infection activated ATF6 pathway.

To determine whether virus infection affected the splicing of XBP-1 transcript, we used RT-PCR to detect XBP-1 splicing in PEDV infected cells from 6 h p.i., and tunicamycin-treated cells were used as the control (Fig. 2E). The result demonstrated that PEDV infection increased the levels of active XBP-1 mRNA.

To determine whether other chaperone genes were activated during PEDV infection, we analyzed the mRNA levels of specific chaperones of ER stress in the total cellular RNA extracted at different time-points (2, 6, 12, 24 and 48 h) after virus infection using quantitative RT-PCR. The housekeeping gene GAPDH was used as the internal control. As shown in Fig. 3, the increased gene expression was observed in all of the studied genes. At 48 h.p.i., the increased transcript levels of GRP78 were consistent with previous Western blot analysis. The transcript levels of GRP94 and ATF4 attenuated from 2 h.p.i. to 12 h.p.i. and increased from 12 h.p.i. to 48 h.p.i. Other UPR-related genes, such as CHOP, GADD34, EDEM, Calr, P58^{IPK}, ERP57, Caln and PDI shared the similar kinetics as GRP78. Taken together, PEDV activated all the three UPR pathways during virus infection from 12 h.p.i.

3.3. Live virus infection is required for UPR induction

To further analyze whether the PEDV replication was required for induction of UPR, we inactivated PEDV by ultraviolet (UV) irradiation and examined its capability of inducing UPR. UV irradiation block viral RNA synthesis and protein synthesis, but has no effects on virus binding to the receptor(s) and its subsequent entry into

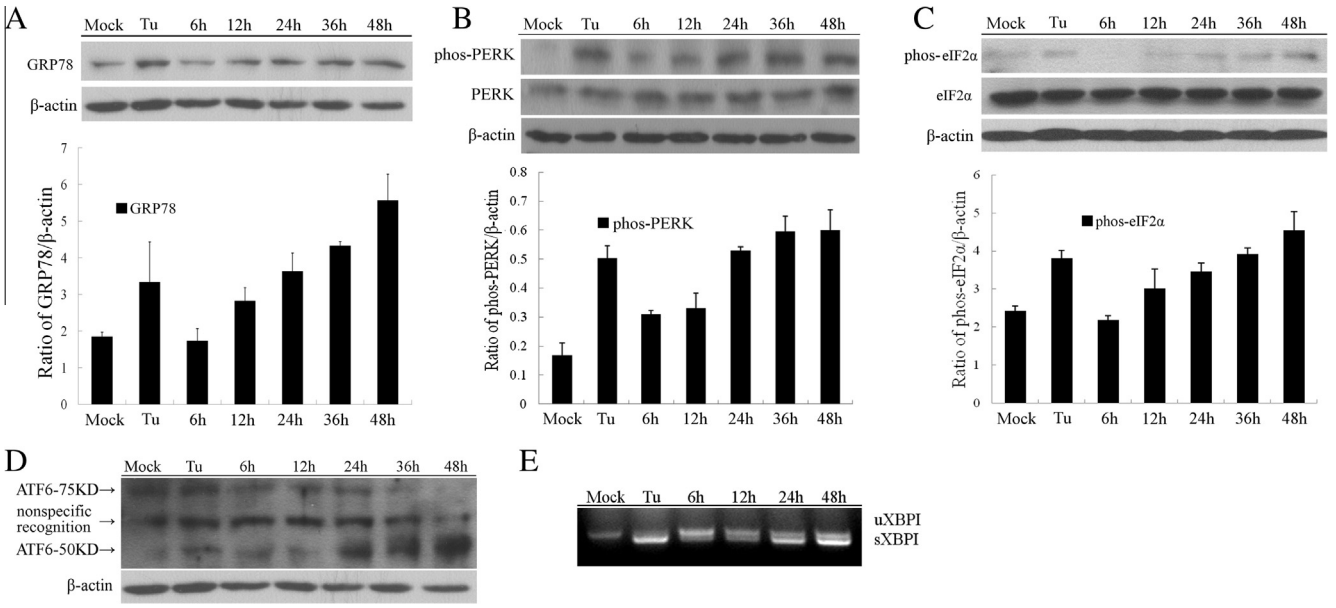

Fig. 2. PEDV induces the host cellular UPR signaling pathways. Vero cells were infected with PEDV at MOI of 0.01 or treated with Tu, the samples were collected at 0, 6, 12, 24, 36 and 48 h.p.i. (A–C) The expression of GRP78, PERK and eIF2α in the samples was analyzed by Western blot. β-Actin was used as sample loading control. (D) The cleavage of ATF6 during UPR was analyzed by Western blot. (E) Unspliced (uXBP-1) and spliced (sXBP-1) mRNA were analyzed by RT-PCR using specific primer pairs.

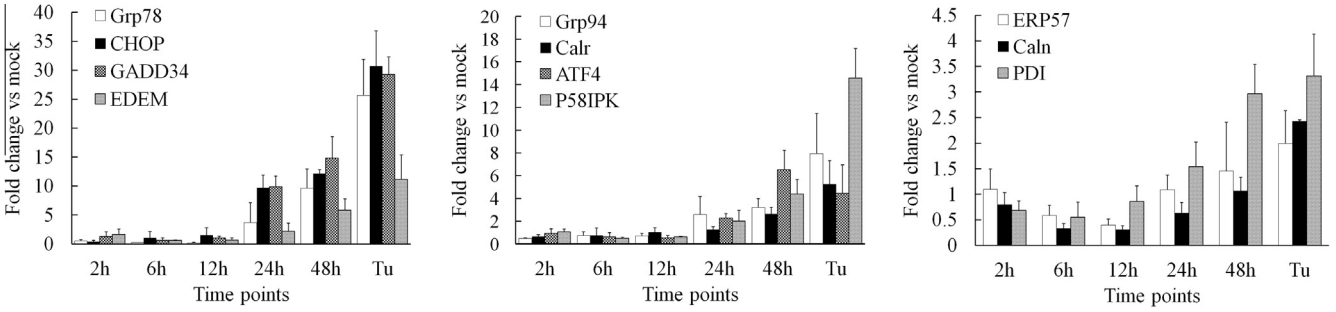

Fig. 3. UPR pathway genes assay. Total RNA was isolated and the transcript levels of the UPR pathway genes were measured by real-time PCR at different time-points (2–48 h) after virus infection. Tu (2 μg/ml) was used as a positive control of UPR activation.

host cells (Beck et al., 1990). Prior to the experiments, the infectivity loss of UV-inactivated viruses was confirmed by Q-PCR assay (data not shown). Cell lysates extracted from PEDV, UV-PEDV-infected Vero cells (Tu treated cells were used as the control) were analyzed by Western blot with antibodies specific to GRP78. As shown in Fig. 4, the expression level of GRP78 in UV-PEDV infected cells was similar to those in mock-infected cells. In contrast, GRP78 expression increased markedly in Vero cells infected with replication-competent PEDV (Fig. 4), suggesting the replication of PEDV is required for the induction of UPR.

3.4. The impairment of UPR increased PEDV replication

To examine the role of UPR in PEDV replication, we silenced the expression of PERK using shRNA interference and reduced PERK expression was confirmed by Western blot. Meanwhile, eIF2α phosphorylation decreased in PERK shRNA treated cells compared with that in the scramble shRNA treated cells (Fig. 5A). Western blot analysis on PEDV N protein showed virus replication was increased in PERK knockdown cells, and the viral titer in supernatant was also increased (Fig. 5B). To further confirm this finding, we evaluated the RNA level of PEDV ORF3 gene in the infected cells by Q-PCR. As shown in Fig. 5C, the RNA level of PEDV ORF3 gene

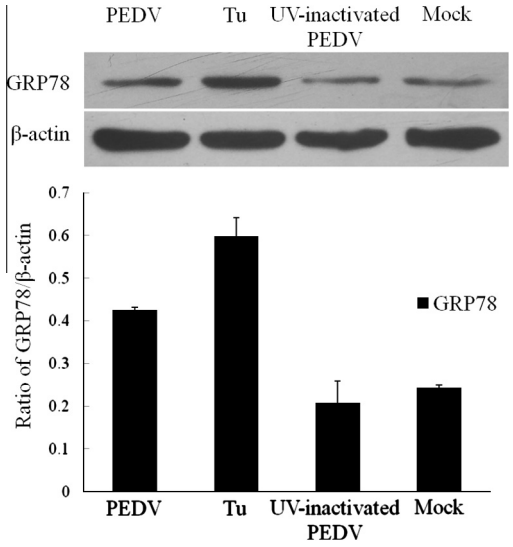

Fig. 4. PEDV replication is required for UPR induction. Vero cells were infected with UV-inactivated PEDV, PEDV (both MOI = 0.01) or treated with Tu (2 μg/ml). The cells were harvested at 24 h and Western blot was performed to determine UPR activation using anti-GRP78 antibody. β-Actin was used as a loading control.

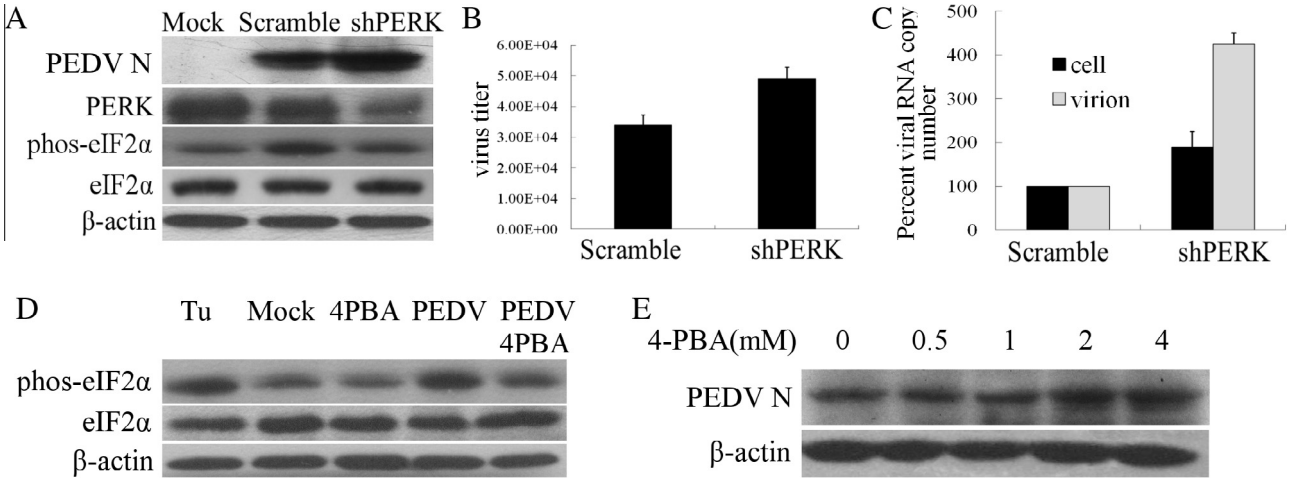

Fig. 5. The impairment of UPR increased PEDV replication. (A) Vero cells were transfected with shRNAs to knockdown protein PERK for 48 h, and then infected with PEDV for 36 h. Scramble shRNA plasmid was used as the negative control. PERK, eIF2α and phos-eIF2α expression and the N protein of PEDV were analyzed by Western blot. β-Actin was used as sample loading control. (B) PEDV titers in the supernatants were measured by plaque formation assays. (C) The RNA level of gene ORF3 from the infected cells was evaluated by Q-PCR. (D, E) Vero cells were infected with PEDV for 2 h, then treated with 4-PBA for 24 h. The Western blot was performed to test eIF2α and phospho-eIF2α expression and the change of N protein of PEDV. β-Actin was used as sample loading control.

increased by 1.8-fold in shPERK treated cells compare with that in scramble shRNA treated cells.

4-Phenyl butyric acid (PBA) is reported to be able to reduce ER stress (Ozcan et al., 2008; Özcan et al., 2006). We next used 4-PBA to determine whether it could affect PEDV replication. As shown in Fig. 5D, 4-PBA decreased the phosphorylation of eIF2α in PEDV infected cells, suggesting 4-PBA alleviated ER stress induced by PEDV infection. Since 4-PBA treatment could decrease the phosphorylation of eIF2α, Vero cells were treated with different concentrations of 4-PBA at 2 h after virus infection. The result showed that virus replication increased after 4-PBA treatment as assayed by Western blot analysis of PEDV N protein (Fig. 5E). Collectively, these data revealed that impairment of UPR either by silencing PERK or 4-PBA treatment attenuated eIF2α phosphorylation and improved the capacity of PEDV replication.

3.5. 2-DG inhibits PEDV replication and gene expression

2-DG is known as an inhibitor of glycolysis, due to its similar structure to mannose. It can induce ER stress via affecting N-linked glycosylation (Leung et al., 2012; Wang et al., 2011). To analyze whether 2-DG exposure triggered UPR in Vero cells, the cells were exposed to 2-DG. The expression level of GRP78 was determined at different time points. As shown in Fig. 6A, GRP78 expression level increased considerably at 6 h, indicating that 2-DG induced ER stress in Vero cells.

To study the impact of 2-DG treatment on PEDV infection, Vero cells were treated with different concentrations of 2-DG for 24 h prior to PEDV infection. The Western blot analysis demonstrated that PEDV N protein in supernatants and the cells decreased in a dose-dependent manner (Fig. 6B). Meanwhile, we determined the viral RNA copy number of mock-treated and 2-DG treated cells at different time points. The ratio between the copy numbers showed that the viral RNA loads were lower in 2-DG treated cells than that in mock-treated cells (Fig. 6C). The viral titers in supernatants monitored by plaque formation assay confirmed the antiviral activity of 2-DG (Fig. 6D). PEDV RNA viral loads in cell and supernatants extracts were decreased as assayed by qPCR (both in supernatants and in cells, Fig. 6E and F), indicating 2-DG inhibited PEDV propagation in a concentration-dependent manner.

3.6. 2-DG treatment affects virus assembly

Since our experiments above showed that 2-DG could inhibit PEDV propagation when the cells were treated with 2-DG prior to the infection, we next tested whether 2-DG treatment affected the expression level of PEDV entry receptor APN (CD13) to impair virus entry. We used flow cytometry to determine CD13 expression level after 2-DG treatment. The result showed that 2-DG treatment increased the expression level of CD13 (Fig. 7A). We next determined whether the increased expression of CD13 could increase the virus entry by RT-PCR and Western blot analysis, and the results showed that 2-DG treatment did not significantly affect virus entry (Fig. 7B and C).

To find out whether 2-DG treatment affects viral protein translation after virus entry, we treated the cells with 2-DG after virus entry. Western blot analysis suggested that 2-DG decreased viral protein translation, implying that 2-DG might affect virus replication at the early stage of virus infection (Fig. 7D).

In order to find out if 2-DG treatment affects virus assembly or release, the Vero cells were treated with 2-DG after they were infected with the virus (MOI = 0.01). PEDV RNA copy numbers of the cell lysates and the supernatants were detected by Q-PCR, the ratios of RNA copy numbers between cell lysates and supernatants treated with 2-DG decreased compared to the control cells in a concentration-dependent manner (Fig. 7E), indicating that 2-DG affected the virus assembly. Meanwhile, the ratios of PEDV titers between the supernatants and the cell lysates was the same between 2-DG treated cells and the control cells ($p > 0.05$) (Fig. 7F), indicating that 2-DG did not affect the virus release (Xu et al., 2012).

4. Discussion

During the course of the virus infection cycle, a large amount of viral proteins are synthesized in infected cells. The accumulation of unfolded or misfolded proteins tends to activate the ER stress response to alleviate the burden. Several studies have shown that in some cases UPR might be beneficial for virus replication, such as in WNV_{KUN}, HCMV and HCV infection (Ambrose and Mackenzie, 2011; Isler et al., 2005; Tardif et al., 2002).

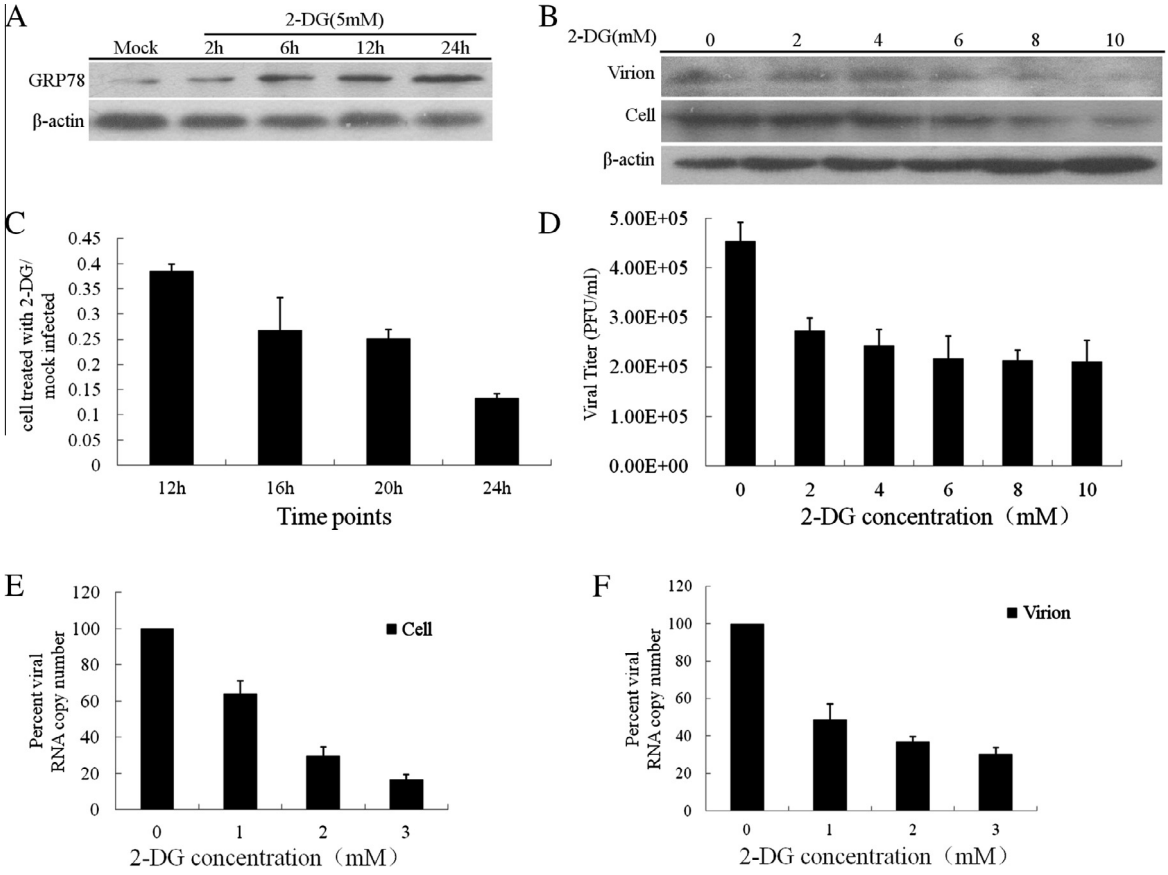

Fig. 6. 2-DG inhibits PEDV replication and gene expression. (A) Vero cells were treated with 5 mM 2-DG for the indicated time. Cell lysates were analyzed by Western blot using antibody against GRP78. (B) Vero cells were infected with PEDV (MOI = 0.01) after pretreated with 2-DG 24 h for indicated concentrations. Supernatant (virions) and cell lysates were analyzed by Western blot using antibody against PEDV N. (C) 2-DG affected PEDV replication. The cells were incubated either in the presence or absence of 2-DG for 24 h before infected with PEDV (MOI = 1). The cells were harvested for the indicated time for RT-PCR analysis using primers specific for PEDV N gene. The ratio was the gene copy number of N gene in 2-DG treated and mock-treated cells. (D) Vero cells were infected with PEDV (MOI = 0.01) for 48 h after cells treated with various dosages of 2-DG for 24 h. PEDV titers in the supernatants were measured by plaque formation assays. (E, F) 5×10^5 Vero cells were infected with PEDV (MOI = 0.01) for 48 h after cells treated with various dosages of 2-DG for 24 h. Total RNA was extracted, and cDNA was synthesized by reverse transcription. The RT-PCR was used to analyze the viral RNA copy numbers in the cells and supernatants (virion).

In the present studies, we confirmed that PEDV infection activated three UPR signal pathways. Interestingly, PEDV attenuated host UPR signal pathways at early time points (0–6 h post-infection), but upregulated them dramatically from 12 h to 48 h. Similar kinetics has been observed in cells infected with arenavirus and HCV (Merquiol et al., 2011; Pasqual et al., 2011). During the infection, the virus must overcome certain aspects of the UPR which are detrimental to viral replication to facilitate their survival.

It has been shown that the phosphorylation of eIF2α leads to the inhibition of protein synthesis in response to diverse stress conditions, including viral infection (He, 2006). Our studies showed that PEDV replication was increased in PERK knockdown cells or 4-PBA treated cells. The higher replication capacity of PEDV in PERK silenced cells might result from their inability to attenuate viral protein synthesis due to an impaired eIF2α phosphorylation. A similar result was observed in PERK$^{-/-}$ MEF cells infected with vesicular stomatitis virus (Baltzis et al., 2004).

2-DG has been used as an ER stress inducer, it also shows antiviral activities against several viruses, including human pathogenic papillomavirus type 18, JC virus and Kaposi's Sarcoma-Associated Herpesvirus (Leung et al., 2012; Maehama et al., 1998; Noch et al., 2012). It has been reported that activation of UPR by 2-DG elicits an early antiviral response via eIF2α inactivation, which impairs protein synthesis required to drive viral replication and oncogenesis (Ke and Chen, 2011). Similar to KSHV (Leung et al., 2012), PEDV also attenuated eIF2α phosphorylation at early time points. It has been shown that 2-DG increased the phosphorylation of eIF2α (DeSalvo et al., 2012; Ramírez-Peinado et al., 2011). Therefore, we suspected that the antiviral activity of 2-DG might be related to the shutdown of viral protein synthesis due to the eIF2α inactivation, as suggested in our Western blot analysis.

In the studies on influenza virus, it is found that 2-DG inhibits the biosynthesis of active hemagglutinin, neuraminidase and mature infectious virions (Kaluza et al., 1972; Kilbourne, 1959). Further studies show that 2-DG prevented the maturation of influenza virus glycoproteins because an unglycosylated or incompletely glycosylated hemagglutinin precursor could be detected (Klenk et al., 1972; Nakamura and Compans, 1978; Schwarz and Klenk, 1974). A study on murine mammary tumor virus shows that 2-DG can completely inhibit the synthesis of viral envelope precursor polyproteins Pr70env, which will be cleaved into two molecules to give rise to mature glycoproteins gp52 and gp36. Meanwhile, pr73 gag was only inhibited by 10–15% by 2-DG (Sarkar, 1986). The native M protein has been shown to be incorporated into PEDV virions in its N-glycosylated form (Utiger et al., 1995). The predicted polypeptide of PEDV spike protein contained 29 potential N-linked glycosylation sites with similar structural features to those of the coronavirus spike protein (Duarte and Laude, 1994). Our data presented here showed that the virus

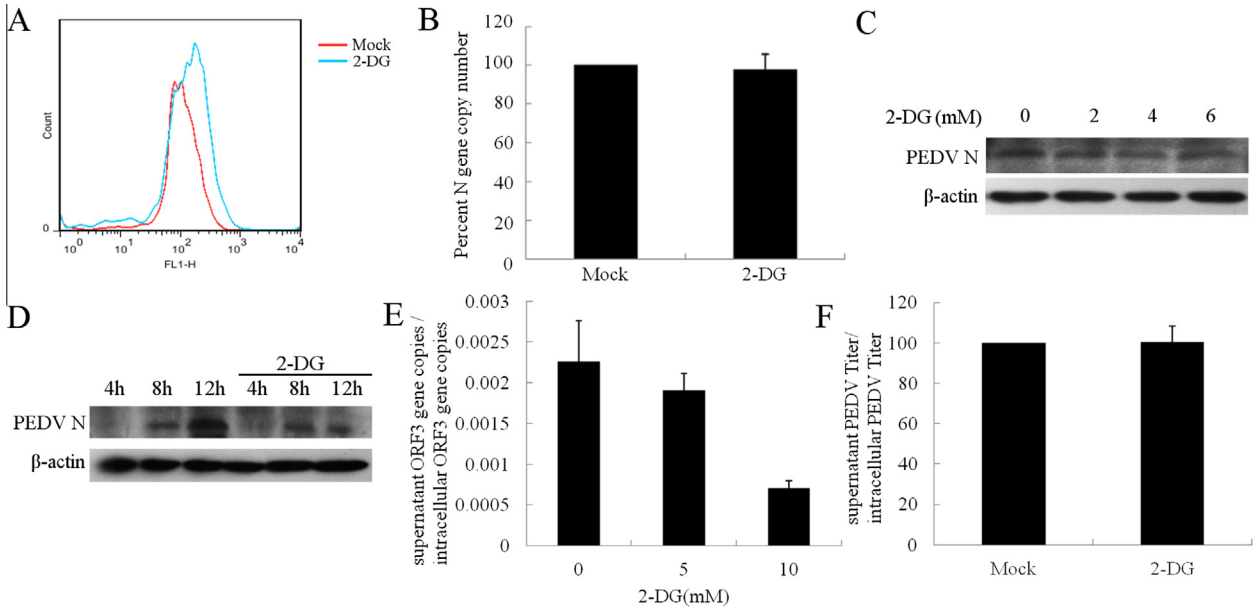

Fig. 7. 2-DG treatment affects virus packaging. (A) Vero cells were pretreated with 10 mM 2-DG for 24 h, and the cells were analyzed by FACS analysis using anti-CD13 polyclonal antibody. (B, C) 2-DG treatment did not affect virus entry as determined by RT-PCR and Western blot analysis. For RT-PCR analysis, the cells were treated with 10 mM 2-DG before virus infection. Bars represent mean percent copy number of viral RNA levels in cells by RT-PCR using primers specific for PEDV N gene. Cell lysates were analyzed by Western blot using antibody against PEDV N. (D) The Vero cells were infected with PEDV for 2 h (MOI = 1), 2-DG (10 mM) was incubated with the cells. The cells were harvested at different time points. Cell lysates were analyzed by Western blot using antibody against PEDV N. (E, F) The Vero cells was treated with different concentrations 2-DG after infected with PEDV (MOI = 0.01) for 2 h, the ratio of PEDV RNA copy numbers between the supernatants and the cell lysates was detected by Q-PCR, and the ratio of the virus titers in supernatants and cell lysates were determined by plaque assay.

assembly in the infected cells could be affected by 2-DG treatment. We suspected that 2-DG treatment might affect the synthesis, folding or glycosylation of viral proteins which subsequently impaired the correct assembly of the virions.

Our result showed that 2-DG leads to UPR activation without causing toxicity in the PEDV-infected cells. At the low and clinically achievable doses used here, 2-DG activation of the UPR has significant anti-PEDV activity, which expanded its potential clinical application as a novel anti-PEDV approach. This study supports the therapeutic potential of using glucose/mannose analogs to induce the UPR and block viral replication.

Acknowledgment

This project was funded by the priority academic program development of Jiangsu Higher Education Institutions.

References

Ambrose, R.L., Mackenzie, J.M., 2011. West Nile virus differentially modulates the unfolded protein response to facilitate replication and immune evasion. J. Virol. 85, 2723–2732.
Baltzis, D., Qu, L.-K., Papadopoulou, S., Blais, J.D., Bell, J.C., Sonenberg, N., Koromilas, A.E., 2004. Resistance to vesicular stomatitis virus infection requires a functional cross talk between the eukaryotic translation initiation factor 2α kinases PERK and PKR. J. Virol. 78, 12747–12761.
Beck, M.A., Chapman, N.M., McManus, B.M., Mullican, J.C., Tracy, S., 1990. Secondary enterovirus infection in the murine model of myocarditis. Pathologic and immunologic aspects. Am. J. Pathol. 136, 669–681.
Bertolotti, A., Zhang, Y., Hendershot, L.M., Harding, H.P., Ron, D., 2000. Dynamic interaction of BiP and ER stress transducers in the unfolded-protein response. Nat. Cell Biol. 2, 326–332.
Buchkovich, N.J., Maguire, T.G., Paton, A.W., Paton, J.C., Alwine, J.C., 2009. The endoplasmic reticulum chaperone BiP/GRP78 is important in the structure and function of the human cytomegalovirus assembly compartment. J. Virol. 83, 11421–11428.
Buchkovich, N.J., Maguire, T.G., Yu, Y., Paton, A.W., Paton, J.C., Alwine, J.C., 2008. Human cytomegalovirus specifically controls the levels of the endoplasmic reticulum chaperone BiP/GRP78, which is required for virion assembly. J. Virol. 82, 31–39.
DeSalvo, J., Kuznetsov, J.N., Du, J., Leclerc, G.M., Leclerc, G.J., Lampidis, T.J., Barredo, J.C., 2012. Inhibition of Akt potentiates 2-DG-induced apoptosis via downregulation of UPR in acute lymphoblastic leukemia. Mol. Cancer Res. 10, 969–978.
Dorner, A., Wasley, L.C., Kaufman, R.J., 1989. Increased synthesis of secreted proteins induces expression of glucose-regulated proteins in butyrate-treated Chinese hamster ovary cells. J. Biol. Chem. 264, 20602–20607.
Duarte, M., Laude, H., 1994. Sequence of the spike protein of the porcine epidemic diarrhoea virus. J. Gen. Virol. 75, 1195–1200.
Fernandez, J., Yaman, I., Sarnow, P., Snider, M.D., Hatzoglou, M., 2002. Regulation of internal ribosomal entry site-mediated translation by phosphorylation of the translation initiation factor eIF2α. J. Biol. Chem. 277, 19198–19205.
Galindo, I., Hernaez, B., Munoz-Moreno, R., Cuesta-Geijo, M.A., Dalmau-Mena, I., Alonso, C., 2012. The ATF6 branch of unfolded protein response and apoptosis are activated to promote African swine fever virus infection. Cell Death Dis. 3, e341.
Hancock, M.H., Cliffe, A.R., Knipe, D.M., Smiley, J.R., 2010. Herpes simplex virus VP16, but not ICP0, is required to reduce histone occupancy and enhance histone acetylation on viral genomes in U2OS osteosarcoma cells. J. Virol. 84, 1366–1375.
He, B., 2006. Viruses, endoplasmic reticulum stress, and interferon responses. Cell Death Differ. 13, 393–403.
Huang, Y.-W., Dickerman, A.W., Piñeyro, P., Li, L., Fang, L., Kiehne, R., Opriessnig, T., Meng, X.-J., 2013. Origin, evolution, and genotyping of emergent porcine epidemic diarrhea virus strains in the United States. mBio 4, e00737–e00713.
Isler, J.A., Skalet, A.H., Alwine, J.C., 2005. Human cytomegalovirus infection activates and regulates the unfolded protein response. J. Virol. 79, 6890–6899.
Jheng, J.R., Lau, K.S., Tang, W.F., Wu, M.S., Horng, J.T., 2010. Endoplasmic reticulum stress is induced and modulated by enterovirus 71. Cell. Microbiol. 12, 796–813.
Kaluza, G., Scholtissek, C., Rott, R., 1972. Inhibition of the multiplication of enveloped RNA-viruses by glucosamine and 2-deoxy-D-glucose. J. Gen. Virol. 14, 251–259.
Ke, P.Y., Chen, S.S., 2011. Activation of the unfolded protein response and autophagy after hepatitis C virus infection suppresses innate antiviral immunity in vitro. J. Clin. Invest. 121, 37–56.
Kilbourne, E.D., 1959. Inhibition of influenza virus multiplication with a glucose antimetabolite (2-deoxy-D-glucose). Nature 183, 271–272.
Klenk, H.-D., Scholtissek, C., Rott, R., 1972. Inhibition of glycoprotein biosynthesis of influenza virus by D-glucosamine and 2-deoxy-D-glucose. Virology 49, 723–734.
Kocherhans, R., Bridgen, A., Ackermann, M., Tobler, K., 2001. Completion of the porcine epidemic diarrhoea coronavirus (PEDV) genome sequence. Virus Genes 23, 137–144.
Kurtoglu, M., Gao, N., Shang, J., Maher, J.C., Lehrman, M.A., Wangpaichitr, M., Savaraj, N., Lane, A.N., Lampidis, T.J., 2007a. Under normoxia, 2-deoxy-D-glucose elicits cell death in select tumor types not by inhibition of glycolysis but by interfering with N-linked glycosylation. Mol. Cancer Ther. 6, 3049–3058.

Kurtoglu, M., Maher, J.C., Lampidis, T.J., 2007b. Differential toxic mechanisms of 2-deoxy-D-glucose versus 2-fluorodeoxy-D-glucose in hypoxic and normoxic tumor cells. Antioxid. Redox Signal. 9, 1383–1390.

Leung, H.J., Duran, E.M., Kurtoglu, M., Andreansky, S., Lampidis, T.J., Mesri, E.A., 2012. Activation of the unfolded protein response by 2-deoxy-D-glucose inhibits Kaposi's sarcoma-associated herpesvirus replication and gene expression. Antimicrob. Agents Chemother. 56, 5794–5803.

Liu, J., HuangFu, W.-C., Kumar, K., Qian, J., Casey, J.P., Hamanaka, R.B., Grigoriadou, C., Aldabe, R., Diehl, J.A., Fuchs, S.Y., 2009. Virus-induced unfolded protein response attenuates antiviral defenses via phosphorylation-dependent degradation of the type I interferon receptor. Cell Host Microbe 5, 72–83.

Maehama, T., Patzelt, A., Lengert, M., Hutter, K.J., Kanazawa, K., Zur Hausen, H., Rösl, F., 1998. Selective down-regulation of human papillomavirus transcription by 2-deoxyglucose. Int. J. Cancer 76, 639–646.

Merquiol, E., Uzi, D., Mueller, T., Goldenberg, D., Nahmias, Y., Xavier, R.J., Tirosh, B., Shibolet, O., 2011. HCV causes chronic endoplasmic reticulum stress leading to adaptation and interference with the unfolded protein response. PLoS One 6, e24660.

Mole, B., 2013. Deadly pig virus slips through US borders. Nature 499, 388.

Nakamura, K., Compans, R.W., 1978. Effects of glucosamine, 2-deoxyglucose, and tunicamycin on glycosylation, sulfation, and assembly of influenza viral proteins. Virology 84, 303–319.

Noch, E., Sariyer, I.K., Gordon, J., Khalili, K., 2012. JC virus T-antigen regulates glucose metabolic pathways in brain tumor cells. PLoS One 7, e35054.

Ozcan, U., Ozcan, L., Yilmaz, E., Düvel, K., Sahin, M., Manning, B.D., Hotamisligil, G.S., 2008. Loss of the tuberous sclerosis complex tumor suppressors triggers the unfolded protein response to regulate insulin signaling and apoptosis. Mol. Cell 29, 541–551.

Özcan, U., Yilmaz, E., Özcan, L., Furuhashi, M., Vaillancourt, E., Smith, R.O., Görgün, C.Z., Hotamisligil, G.S., 2006. Chemical chaperones reduce ER stress and restore glucose homeostasis in a mouse model of type 2 diabetes. Science 313, 1137–1140.

Park, S.J., Kim, H.K., Song, D.S., Moon, H.J., Park, B.K., 2011. Molecular characterization and phylogenetic analysis of porcine epidemic diarrhea virus (PEDV) field isolates in Korea. Arch. Virol. 156, 577–585.

Pasqual, G., Burri, D.J., Pasquato, A., de la Torre, J.C., Kunz, S., 2011. Role of the host cell's unfolded protein response in arenavirus infection. J. Virol. 85, 1662–1670.

Pensaert, M., De Bouck, P., 1978. A new coronavirus-like particle associated with diarrhea in swine. Arch. Virol. 58, 243–247.

Ramírez-Peinado, S., Alcázar-Limones, F., Lagares-Tena, L., El Mjiyad, N., Caro-Maldonado, A., Tirado, O.M., Muñoz-Pinedo, C., 2011. 2-Deoxyglucose induces Noxa-dependent apoptosis in alveolar rhabdomyosarcoma. Cancer Res. 71, 6796–6806.

Rutkowski, D.T., Arnold, S.M., Miller, C.N., Wu, J., Li, J., Gunnison, K.M., Mori, K., Sadighi Akha, A.A., Raden, D., Kaufman, R.J., 2006. Adaptation to ER stress is mediated by differential stabilities of pro-survival and pro-apoptotic mRNAs and proteins. PLoS Biol. 4, e374.

Sarkar, N.H., 1986. The effects of 2-deoxyglucose and tunicamycin on the biosynthesis of the murine mammary tumor virus proteins, and on the assembly and release of the virus. Virology 150, 419–438.

Schwarz, R.T., Klenk, H.-D., 1974. Inhibition of glycosylation of the influenza virus hemagglutinin. J. Virol. 14, 1023–1034.

Song, D., Park, B., 2012. Porcine epidemic diarrhoea virus: a comprehensive review of molecular epidemiology, diagnosis, and vaccines. Virus Genes 44, 167–175.

Sung, S.-C., Chao, C.-Y., Jeng, K.-S., Yang, J.-Y., Lai, M., 2009. The 8ab protein of SARS-CoV is a luminal ER membrane-associated protein and induces the activation of ATF6. Virology 387, 402–413.

Tardif, K.D., Mori, K., Siddiqui, A., 2002. Hepatitis C virus subgenomic replicons induce endoplasmic reticulum stress activating an intracellular signaling pathway. J. Virol. 76, 7453–7459.

Utiger, A., Tobler, K., Bridgen, A., Ackermann, M., 1995. Identification of the membrane protein of porcine epidemic diarrhea virus. Virus Genes 10, 137–148.

Wang, Q., Liang, B., Shirwany, N.A., Zou, M.-H., 2011. 2-Deoxy-D-glucose treatment of endothelial cells induces autophagy by reactive oxygen species-mediated activation of the AMP-activated protein kinase. PLoS One 6, e17234.

Wood, E.N., 1977. An apparently new syndrome of porcine epidemic diarrhoea. Vet. Rec. 100, 243–244.

Xu, S., Pei, R., Guo, M., Han, Q., Lai, J., Wang, Y., Wu, C., Zhou, Y., Lu, M., Chen, X., 2012. Cytosolic phospholipase A2 gamma is involved in hepatitis C virus replication and assembly. J. Virol. 86, 13025–13037.

Xu, X., Zhang, H., Zhang, Q., Dong, J., Liang, Y., Huang, Y., Liu, H.J., Tong, D., 2013a. Porcine epidemic diarrhea virus E protein causes endoplasmic reticulum stress and up-regulates interleukin-8 expression. Virol. J. 10, 26.

Xu, X., Zhang, H., Zhang, Q., Huang, Y., Dong, J., Liang, Y., Liu, H.J., Tong, D., 2013b. Porcine epidemic diarrhea virus N protein prolongs S-phase cell cycle, induces endoplasmic reticulum stress, and up-regulates interleukin-8 expression. Vet. Microbiol. 164, 212–221.

Ye, J., Rawson, R.B., Komuro, R., Chen, X., Davé, U.P., Prywes, R., Brown, M.S., Goldstein, J.L., 2000. ER stress induces cleavage of membrane-bound ATF6 by the same proteases that process SREBPs. Mol. Cell 6, 1355–1364.

Yoshida, H., Matsui, T., Hosokawa, N., Kaufman, R.J., Nagata, K., Mori, K., 2003. A time-dependent phase shift in the mammalian unfolded protein response. Dev. Cell 4, 265–271.

Yu, C., Achazi, K., Niedrig, M., 2013. Tick-borne encephalitis virus triggers inositol-requiring enzyme 1 (IRE1) and transcription factor 6 (ATF6) pathways of unfolded protein response. Virus Res. 178, 471–477.

Zhang, L., Wang, A., 2012. Virus-induced ER stress and the unfolded protein response. Front. Plant Sci. 3, 293.